Pattern formation and instability in a kinetic chemotaxis model

Shugo YASUDA
Graduate School of Simulation Studies, University of Hyogo, Kobe 650-0047, Japan

I. INTRODUCTION

Collective motion of chemotactic bacteria such as *Escherichia Coli* relies on a continuous reorientation by runs and tumbles at the individual level [1, 2]. It is known that the rate of tumble λ (or the length of run $V_0\lambda^{-1}$, where V_0 is the running speed of bacteria) is modulated by a stiff response to a temporal sensing of extracellular chemical cue S along the pathway. In the temporal sensing, if the chemical concentration steeply increases (or decreases) in time as a step function, bacteria rapidly decrease (or increase) their tumbling rate and, after an adaptation period, they return their tumbling rate to the basal tumbling rate λ_0.

If we consider the fast adaptation (although this is not always true in general), the tumbling rate can be described by a function of the temporal derivative of chemical cue along the pathway [3–5] as

$$\lambda = \lambda_0 \left[1 - F_\delta \left(D_t \log S|_{\mathbf{v}}\right)\right], \tag{1}$$

where $F_\delta(X)$ is the response function defined as

$$F_\delta(X) = F\left(\frac{X}{\delta}\right), \quad F'(X) > 0, \quad F(X) \to \pm\chi \quad \text{as } X \to \pm\infty, \tag{2}$$

and $D_t S|_{\boldsymbol{v}}$ is the material derivative of the concentration of chemical cues $S(t, \boldsymbol{x})$ along the bacteria velocity $\boldsymbol{v}$, i.e.,

$$D_t S|_{\boldsymbol{v}} = \partial_t S + \boldsymbol{v} \cdot \nabla S. \tag{3}$$

In Equation (2), we consider the stiff and bounded function for the chemotactic response, where δ and χ represent the stiffness and modulation amplitude, respectively. We also note that in Equation (1), the logarithmic sensing, which was reported in experiment [6], is considered.

With using the response function, the density of chemotactic bacteria with velocity $\boldsymbol{v} = (v_x, v_y, v_z) \in V$ at position $\boldsymbol{x} = (x, y, z) \in \mathbb{R}^3$ and time $t \geq 0$, $f(t, \boldsymbol{x}, \boldsymbol{v})$ can be described by the following kinetic transport equation,

$$\partial_t f(t, \boldsymbol{x}, \boldsymbol{v}) + \boldsymbol{v} \cdot \nabla f = \frac{1}{k}\left\{\int_V K(D_t \log S|_{\boldsymbol{v}'}) f(\boldsymbol{v}') d\boldsymbol{v}' - K(D_t \log S|_{\boldsymbol{v}}) f(\boldsymbol{v})\right\} + P(\rho) f(\boldsymbol{v}), \tag{4}$$

where the velocity space V is the surface of the ball with $|V| = 1$, ρ is the population density calculated by

$$\rho(t, \boldsymbol{x}) = \int_V f(t, \boldsymbol{x}, \boldsymbol{v}) d\boldsymbol{v}, \tag{5}$$

and $P(\rho)$ is the population-growth rate dependent on the local population density ρ as

$$P(\rho) = \begin{cases} > 0 & (0 \leq \rho < 1), \\ < 0 & (1 < \rho), \\ 1 - \rho & \text{for } \rho \simeq 1. \end{cases} \tag{6}$$

Here, k represents the mean run length of bacteria $V_0\lambda_0^{-1}$ scaled by a characteristic length L_0. The chemical concentration S is described by the following equation,

$$-d\Delta S + S = \rho, \tag{7}$$

where d is the diffusion constant.

Incidentally we note that the kinetic chemotaxis model with the stiff and bounded response, Eqs. (4)–(7) are related to a flux-limited Keller-Segel equation in the continuum limit $k \to 0$ [7–9].

In Ref. [9], the instability analysis of Equations (4)–(7) was carried out for the uniform solution $f = S = 1$ and the following stiffness-induced instability condition was theoretically obtained,

$$\frac{F'_\delta(0)}{k} > \left(1 + \frac{k}{\frac{k\lambda}{\arctan(k\xi)} - 1}\right)(1 + d\xi^2), \tag{8}$$

where $\xi = |\boldsymbol{\xi}|^2$ and $\boldsymbol{\xi}$ is the Fourier variable of $\boldsymbol{x}$. Thus, if the stiffness of the response $F'_\delta(0)$ is sufficiently large, the Fourier mode ξ which satisfies the above equation becomes linearly unstable. Furthermore, it is also proved that the unstable mode ξ is always bounded, i.e., no high frequency oscillation occur. This result indicates that a pattern is always created under the instability condition (8).

The numerical analysis of the pattern formation in a one-dimensional channel with periodic boundaries was also carried out by using the Monte Carlo (MC) code, which was originally developed by the author [10]. The numerical results demonstrated that the instability condition (8) is quite sharp; i.e., the periodic oscillation pattern was always created when the stiffness $F'_\delta(0)$ is slightly above the critical value calculated by the right-hand side of (8) while no oscillatory pattern was observed when the stiffness is just slightly below the critical value. It was also found that the oscillatory pattern changes to the periodic spikes when the modulation amplitude χ increases.

In this paper, the MC method for the kinetic chemotaxis model (4)–(7) is explained in the next section and the numerical results for the two-dimensional pattern formation problems are given in section III.

II. MONTE CARLO METHOD

The motions of the chemotactic bacteria are simulated by using the MC particles which follows the process described by the kinetic chemotaxis equation Eq. (4) coupled with the reaction-diffusion equation for the chemoattractant Eq. (7).

The reaction-diffusion equation Eq. (7) is solved on the $I \times J$ uniform mesh-lattice system with interval Δx by using an usual finite volume scheme. Hereafter, the superscript n and the subscript i represents the time step and the ith lattice site in two dimensional array, respectively, e.g., $S_i^n = S(n\Delta t, \boldsymbol{x}_i)$, where $\boldsymbol{x}_i = (i'\Delta x, j'\Delta x)$ with $i = i' + j'I$ $(0 \le i' < I,\ 0 \le j' < J)$. Here, Δt is the time-step size.

The MC particles are distributed over the $I\Delta x \times J\Delta x$ rectangular domain D. The population density of bacteria in the ith lattice site ρ_i^n is calculated from the number of the MC particles involved in the ith lattice site, M_i^n, as

$$\rho_i^n = M_i^n / M, \tag{9}$$

where M is the number of MC particles involved in one lattice site in the reference state, i.e, $M = N/(I \times J)$, where N is the total number of MC particles in the initial state.

The MC simulation is conducted using the following steps. Hereafter, the position and velocity of the lth particle are expressed as $\boldsymbol{r}_{(l)}^n \in D$ and $\boldsymbol{v}_{(l)}^n \in V$.

1. At $\hat{t} = 0$, MC particles are distributed according to the initial density. In each lattice site, MC particles are distributed uniformly at random positions and their velocities $\boldsymbol{v}$ are determined by the probability density $f_i^0(\boldsymbol{v})/\rho_i^0$.

2. Particles move with their velocities for a duration $\Delta\hat{t}$:

$$\boldsymbol{r}_{(l)}^{n+1} = \boldsymbol{r}_{(l)}^n + \boldsymbol{v}_{(l)}^n \Delta\hat{t} \quad (l = 1, \cdots, N^n), \tag{10}$$

where N^n is the total number of simulation particles at time step n, i.e., $N^n = \sum_{i=0}^{I-1} M_i^n$. The particles that move beyond the boundaries are inserted into the domain D according to the boundary conditions.

3. At each lattice site, the population densities ρ_i^{n+1} and concentrations of chemical cues S_i^{n+1} ($i = 0, \cdots, I-1$) are calculated.

4. The tumbling of each particle is judged using the scattering kernel in Eq. (4). The tumbling of the lth particle may occur with a probability

$$\frac{\Delta t}{k} K[D_t \log S_{(l)}^{n+1}], \tag{11}$$

where $D_t \log S_{(l)}$ represents the temporal variation of the chemical cue experienced by the lth MC particle along the pathway, and is defined by the following forward difference,

$$D_t \log S_{(l)}^n = \frac{\log S(t^n, \boldsymbol{r}_{(l)}^n) - \log S(t^n - \Delta t, \boldsymbol{r}_{(l)}^n - \boldsymbol{v}_{(l)}^n \Delta t)}{\Delta t}. \tag{12}$$

The local concentration of chemical cue at the position of the lth MC particle is calculated by using linear interpolation between the neighboring lattice sites

5. For the particle that is judged to tumble, say the l_tth particle, a new velocity after the tumbling, $\boldsymbol{v}_{(l_t)}^{n+1}$, is determined randomly as,

$$v_x = 1 - 2U_1, \quad v_y = \sqrt{1 - v_x^2}\cos(2\pi U_2), \quad v_z = \sqrt{1 - v_x^2}\sin(2\pi U_2). \tag{13}$$

Here U_1 and U_2 are the uniform random variables between 0 and 1.

6. The divisions/deaths are judged for all MC particles. The division (or death) occurs with a probability $|P[\rho_i^n]|\Delta t$, if $|P[\rho_i^n]|$ is positive (or negative), where ρ_i^n is the local population density at the lattice site where each MC particle is involved. For a particle that is judged to undergo division, e.g., the lth particle, a new particle with the same velocity $\boldsymbol{v}_{(l)}$ is created at a random position within the same lattice site. The numbers of MC particles involved in each lattice site are counted, M_i^{n+1} ($i = 0, \cdots, I \times J - 1$), and the total number of simulation particles is updated as N^{n+1}.

7. Return to step (ii) with the obtained $\boldsymbol{r}_{(l)}$, $\boldsymbol{v}_{(l)}$, $S_{(l)}$ (l=1,$\cdots$,M) at the new time step.

In Ref. [9], the weak formulation of the MC method is also presented.

III. NUMERICAL RESULTS FOR TWO-DIMENSIONAL PATTERNS

The MC results of the pattern formation of chemotactic bacteria in a narrow channel and in a square domain are shown in Figure 1 and 2, respectively. In both figures, the parameters are set to satisfy the instability condition (8).

It is obviously seen that the different types of pattern are produced in the different geometries. In the narrow channel, the strip pattern forms while in the square domain, the spot pattern forms. In the narrow channel, the front of the population wave propagates with a constant speed in the beginning. In the square domain, the population radially expand with a constant speed in the beginning. In both figures, it is seen that the patterns form behind the propagating fronts. The result obtained in the narrow channel seems to be consistent with the result of the one-dimensional periodic system obtained in Ref. [9, 11].

The further investigation on the two-dimensional pattern formation in the kinetic chemotaxis model will be reported elsewhere.

Acknowledgments

This study was financially supported byJSPS KAKENHI Grant Number 16K17554.

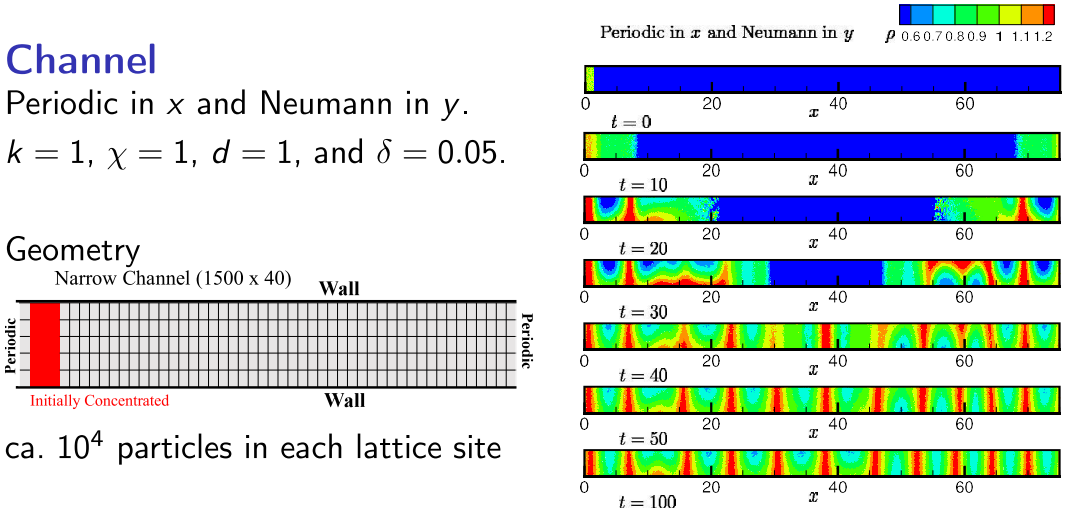

FIG. 1: Strip pattern formation in a narrow channel between parallel walls. The parameters in the kinetic chemotaxis model is set as k=1, χ=1, d=1, and δ=0.05. The rectangular domain is divided into the 1500×40 uniform lattice meshes. The periodic boundary condition is used in x direction while the Neumann boundary condition is used at the walls. (See the left figure.) The bacteria is initially concentrated at the left side of the channel. The right figures show the time evolution of the population density of bacteria in the narrow channel.

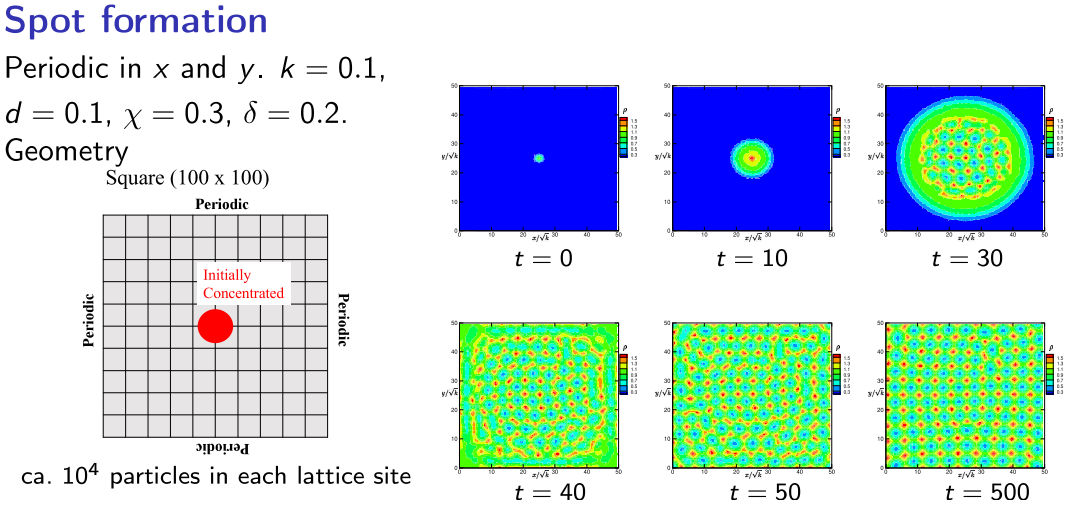

FIG. 2: Spot pattern formation in a square domain with periodic boundaries. The parameters in the kinetic chemotaxis model is set as k=0.1, χ=0.3, d=0.1, and δ=0.2. The square domain is divided into the 100×100 uniform lattice meshes. (See the left figure.) The bacteria is initially concentrated at the center of the domain. The right figures show the time evolution of the population density of bacteria.

References

[1] J. Adler, "Chemotaxis in bacteria", Annu. Rev. Biochem. **44**, 341 (1975).
[2] H. C. Berg, *E. Coli in Motion* (Springer, Berlin, 2003).

[3] R. Erban and H. G. Othmer, "From individual to collective behavior in bacterial chemotaxis", SIAM J. Appl. Math. **65**, 361 (2004).
[4] Y. Dolak and C. Schmeiser, "Kinetic models for chemotaxis: Hydrodynamic limits and spatio-temporal mechanisms", J. Math. Biol. **51**, 595 (2005).
[5] B. Perthame, M. Tang, and N. Vauchelet, "Derivation of the bacterial run-and-tumble kinetic equation from a model with biochemical pathway", J. Math. Biol. **73**, 1161 (2016).
[6] Y. V. Kalinin, L. Jiang, Y. Tu, and M. Wu, "Logarithmic sensing in Escherichia coli bacterial chemotaxis", Biophys. J. **96**, pp. 2439–2448 (2009).
[7] A. Chertock, A. Kurganov, X. Wang, and Y. Wu, "On a chemotaxis model with saturated chemotactic flux", Kinetic and related models **5**, 51–95 (2012).
[8] N. Bellomo and M. Winkler, "A degenerate chemotaxis system with flux limitation: Maximally extended solutions and abasence of gradient blow-up", Commun. Part. Diff. Eq. **42**, 436–473 (2017).
[9] B. Perthame and S. Yasuda, "Stiff-response-induced instability for chemotactic bacteria and flux-limited Keller-Segel equation", Nonlinearity **31**, pp. 4065–4089 (2018).
[10] S. Yasuda, "Monte Carlo simulation for kinetic chemotaxis model: An application to the traveling population wave", J. Comput. Phys. **330**, pp. 1022–1042 (2017).
[11] V. Calvez, B. Perthame, and S. Yasuda, "Traveling wave and aggregation in a flux-limited Keller-Segel model", Kinet. Relat. Mod. **11**, pp. 891-–909 (2018).